

# Analyses of multi-pion Bose-Einstein correlations for the granular sources with coherent pion-emission droplets

Ghulam Bary<sup>1</sup>, Wei-Ning Zhang<sup>1,2\*</sup>, Peng Ru<sup>3</sup>, Jing Yang<sup>4</sup>

<sup>1</sup>*School of Physics, Dalian University of Technology, Dalian, 116024, China*

<sup>2</sup>*School of Physics, Harbin Institute of Technology, Harbin, 150006, China*

<sup>3</sup>*Institute of Quantum Matter, South China Normal University, Guangzhou, 510006, China*

<sup>4</sup>*School of Physics, Changchun Normal University, Changchun, 130032, China*

ALICE Collaboration measured the three- and four-pion Bose-Einstein correlations (BECs) in Pb-Pb collisions at the Large Hadron Collider (LHC). It is speculated that the significant suppressions of multi-pion BECs are due to a considerable degree of coherent pion emission in the collisions. To explain the observed suppressions, we study the multi-pion BEC functions in a granular source model with coherent pion-emission droplets. We find that the intercepts of multi-pion correlation functions at the relative momenta near zero are sensitive to the droplet number in the granular source. They decrease with decreasing droplet number. The model results of three- and four-pion correlation functions are in basic agreement with the experimental data in central Pb-Pb collisions at the LHC. The normalized four-pion correlation function is sensitive to the momentum dependence of emission coherence. Its rise in moderate relative-momentum region is a signal that high-momentum pions are more possibly emitted chaotically compared to low-momentum pions which may condense in the ground state due to identical boson condensation.

PACS numbers: 25.75.-q, 25.75.Gz

## I. INTRODUCTION

Identical pion intensity correlations (Bose-Einstein correlations, BECs) are important observables in high-energy heavy-ion collisions [1–6]. Because the multiplicity of identical pions in heavy-ion collisions at the Large Hadron Collider (LHC) is very high, multi-pion BEC analyses with high statistic accuracy are available [7, 8]. Recently, the ALICE Collaboration measured significant suppressions of three-pion and four-pion BECs in Pb-Pb collisions at  $\sqrt{s_{NN}} = 2.76$  TeV at LHC [7, 8], which indicates that there may exist a considerable coherence degree for the particle-emitting sources produced in the collisions [7–11].

Analyses of multi-pion BECs can provide more information of the particle-emitting sources compared to two-pion interferometry [4, 5, 7–26]. In particular, multi-pion BECs are sensitive to the source coherence [9–12, 20]. In Refs. [10, 11], we investigated the three- and four-pion BECs for a spherical evolving source of pion gas with identical boson condensation. However, the particle-emitting sources produced in relativistic heavy-ion collisions are anisotropic in space and may have complex structure. It is of interest to explain the experimental measurements of multi-pion BEC suppressions at the LHC based on a more realistic model that can also explain the other observables in the collisions.

On event-by-event basis, the initial systems produced in relativistic heavy-ion collisions are highly fluctuated in space. This initial fluctuation may lead to an inhomogeneous particle-emitting source, in which there are

hot spots and cold valleys. In Refs. [27–30], a granular source model was proposed and developed by W. N. Zhang et al. to explain the experimental results of two-pion interferometry at the Relativistic Heavy Ion Collider (RHIC) and LHC [31–33]. In Refs. [34–36], the granular source model was used to systemically study the pion transverse-momentum spectra, elliptic flows, and two-pion BECs in heavy-ion collisions at the RHIC and LHC. The granular source model can reproduce the experimental data of pion transverse-momentum spectrum, elliptic flow, and two-pion interferometry radii [34–36]. Considering identical pions are emitted from the droplets in the granular source model and the droplet radii are much smaller than the source size, the pion emission from one droplet is perhaps coherent in the case of high pion event multiplicity due to the condensation of identical bosons [10, 11, 37, 38].

In this work, we consider a granular source with coherent pion-emission droplets. The droplets in the granular source move with anisotropic velocities and evolve in viscous hydrodynamics, as described in Ref. [36]. However, identical pion emission from one droplet are assumed to be completely or partially coherent. We investigate the multi-pion BECs in the granular source model with coherent pion-emission droplets. The normalized three- and four-pion correlation functions of the granular sources are examined for completely coherent and momentum-dependent partially coherent pion emissions from a droplet.

The rest parts of this paper is organized as follows. In Sec. II, we examine the three- and four-pion BEC functions of a static granular source with coherent pion-emission droplets. In Sec. III, we investigate the three-pion and four-pion BECs in the granular source model in which the droplets evolve in viscous hydrodynamics.

---

\*wnzhang@dlut.edu.cn

We also investigate the normalized multi-pion correlation functions of the evolving granular sources in this section. Finally, we give a summary and discussion in Sec. IV.

## II. MULTI-PION BECS OF STATIC GRANULAR SOURCES

We first consider a static granular source where identical pions are emitted from separated droplets. The spa-

tial distribution of the emitting-points in each droplet is assumed with a Gaussian distribution  $\sim e^{r^2/(2r_d^2)}$ , and the droplet centers  $R_j$  ( $j = 1, 2, \dots, n$ ) distribute in the granular source with a Gaussian distribution  $\sim e^{-R_j^2/2R_G^2}$ . The two-pion and three-pion BEC functions of the static granular source can be expressed as [39, 40]

$$C_2(\mathbf{p}_1, \mathbf{p}_2) = 1 + \frac{1}{n} e^{-q_{12}^2 r_d^2} + \left(1 - \frac{1}{n}\right) e^{-q_{12}^2 (r_d^2 + R_G^2)} \equiv 1 + \frac{1}{n} \mathcal{R}^d(1, 2) + \left(1 - \frac{1}{n}\right) \mathcal{R}^G(1, 2), \quad (1)$$

$$\begin{aligned} C_3(\mathbf{p}_1, \mathbf{p}_2, \mathbf{p}_3) = & 1 + \frac{1}{n} \left[ \mathcal{R}^d(1, 2) + \mathcal{R}^d(1, 3) + \mathcal{R}^d(2, 3) \right] + \left(1 - \frac{1}{n}\right) \left[ \mathcal{R}^G(1, 2) + \mathcal{R}^G(1, 3) + \mathcal{R}^G(2, 3) \right] \\ & + \frac{2}{n^2} \left[ \mathcal{R}^d(1, 2) \mathcal{R}^d(1, 3) \mathcal{R}^d(2, 3) \right]^{\frac{1}{2}} + \frac{2(n-1)}{n^2} \left[ \left( \mathcal{R}^d(1, 3) \mathcal{R}^d(2, 3) / \mathcal{R}^d(1, 2) \right)^{\frac{1}{2}} \mathcal{R}^G(1, 2) \right. \\ & + \left. \left( \mathcal{R}^d(1, 2) \mathcal{R}^d(2, 3) / \mathcal{R}^d(1, 3) \right)^{\frac{1}{2}} \mathcal{R}^G(1, 3) + \left( \mathcal{R}^d(1, 2) \mathcal{R}^d(1, 3) / \mathcal{R}^d(2, 3) \right)^{\frac{1}{2}} \mathcal{R}^G(2, 3) \right] \\ & + \frac{2(n-1)(n-2)}{n^2} \left[ \mathcal{R}^G(1, 2) \mathcal{R}^G(1, 3) \mathcal{R}^G(2, 3) \right]^{\frac{1}{2}}, \end{aligned} \quad (2)$$

where  $n$  is the droplet number in the granular source,  $\mathcal{R}^d(1, 2) = e^{-q_{12}^2 r_d^2}$ ,  $\mathcal{R}^G(1, 2) = e^{-q_{12}^2 (r_d^2 + R_G^2)}$ , and  $q_{12} = |\mathbf{p}_1 - \mathbf{p}_2|$ . In Eq. (1), the  $\mathcal{R}^d(1, 2)$  and  $\mathcal{R}^G(1, 2)$  terms express the correlations of two pions emitted from one droplet and different droplets, respectively. In Eq. (2), the  $\frac{2}{n^2}[\dots]$  and  $\frac{2(n-1)}{n^2}[\dots]$  terms express the pure triplet correlations of three pions emitted from one droplet and where two pions emitted from one droplet, respectively. In Eq. (2), the last term expresses the pure triplet correlations of three pions emitted from different droplets. The two-pion and three-pion correlation functions be-

come those of the Gaussian sources when  $n = 1$  and  $n \rightarrow \infty$  ( $r_d \rightarrow 0$ ).

For a small droplet radius, the pion emission from a droplet is significantly coherent [10, 11, 37, 38]. Assuming the pions emitted from one droplet are completely coherent, the two-pion and three-pion correlation functions of the granular source become

$$C_2(\mathbf{p}_1, \mathbf{p}_2) = 1 + \frac{(n-1)}{n} \mathcal{R}^G(1, 2), \quad (3)$$

$$C_3(\mathbf{p}_1, \mathbf{p}_2, \mathbf{p}_3) = 1 + \frac{(n-1)}{n} \left[ \mathcal{R}^G(1, 2) + \mathcal{R}^G(1, 3) + \mathcal{R}^G(2, 3) \right] + \frac{2(n-1)(n-2)}{n^2} \left[ \mathcal{R}^G(1, 2) \mathcal{R}^G(1, 3) \mathcal{R}^G(2, 3) \right]^{\frac{1}{2}}. \quad (4)$$

The four-pion correlation function of the granular source with completely coherent pion-emission droplets can be expressed as

$$\begin{aligned} C_4(\mathbf{p}_1, \mathbf{p}_2, \mathbf{p}_3, \mathbf{p}_4) = & 1 + \frac{(n-1)}{n} \left[ \mathcal{R}^G(1, 2) + \mathcal{R}^G(1, 3) + \mathcal{R}^G(1, 4) + \mathcal{R}^G(2, 3) + \mathcal{R}^G(2, 4) + \mathcal{R}^G(3, 4) \right] \\ & + \frac{2(n-1)(n-2)}{n^2} \left[ \left( \mathcal{R}^G(1, 2) \mathcal{R}^G(1, 3) \mathcal{R}^G(2, 3) \right)^{\frac{1}{2}} + \left( \mathcal{R}^G(1, 2) \mathcal{R}^G(1, 4) \mathcal{R}^G(2, 4) \right)^{\frac{1}{2}} \right. \\ & + \left. \left( \mathcal{R}^G(2, 3) \mathcal{R}^G(2, 4) \mathcal{R}^G(3, 4) \right)^{\frac{1}{2}} + \left( \mathcal{R}^G(1, 3) \mathcal{R}^G(1, 4) \mathcal{R}^G(3, 4) \right)^{\frac{1}{2}} \right] \\ & + \frac{(n-1)^2}{n^2} \left[ \mathcal{R}^G(1, 2) \mathcal{R}^G(3, 4) + \mathcal{R}^G(1, 3) \mathcal{R}^G(2, 4) + \mathcal{R}^G(2, 3) \mathcal{R}^G(1, 4) \right] \end{aligned}$$

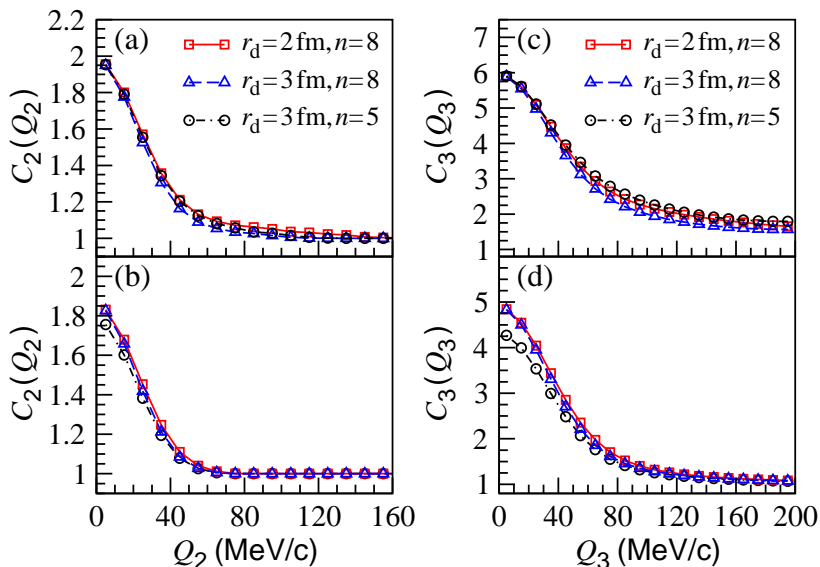


FIG. 1: (Color online) Two-pion and three-pion correlation functions of the static granular source with chaotic [panels (a) and (c)] and completely coherent [panels (b) and (d)] pion-emission droplets. Here, the radii of the granular sources are taken to be  $R_G = 6.0$  fm.

$$\begin{aligned}
& + \frac{2(n-1)(n-2)(n-3)}{n^3} \left[ \left( \mathcal{R}^G(1,2)\mathcal{R}^G(2,3)\mathcal{R}^G(3,4)\mathcal{R}^G(1,4) \right)^{\frac{1}{2}} \right. \\
& \left. + \left( \mathcal{R}^G(1,3)\mathcal{R}^G(2,3)\mathcal{R}^G(2,4)\mathcal{R}^G(1,4) \right)^{\frac{1}{2}} + \left( \mathcal{R}^G(1,2)\mathcal{R}^G(2,4)\mathcal{R}^G(3,4)\mathcal{R}^G(1,3) \right)^{\frac{1}{2}} \right], \quad (5)
\end{aligned}$$

where the last two terms  $\frac{(n-1)^2}{n^2}[\dots]$  and  $\frac{2(n-1)(n-2)(n-3)}{n^3}[\dots]$  are for the correlations of double pion pair and pure pion-quadruplet interference, respectively.

In Figs. 1(a) and 1(b), we plot the two-pion correlation functions of the static granular sources with chaotic and completely coherent pion-emission droplets, respectively. In Figs. 1(c) and 1(d), we plot the three-pion correlation functions of the static granular sources with chaotic and completely coherent pion-emission droplets, respectively. Here, the radii of the granular sources are taken to be  $R_G = 6.0$  fm. The variable  $Q_m$  ( $m = 2, 3, \dots$ ) is defined by the covariant relative momenta, as

$$Q_m = \sqrt{\sum_{i < j \leq m} -(p_i - p_j)^\mu (p_i - p_j)_\mu}, \quad (m \geq 2). \quad (6)$$

From Fig. 1 it can be seen that the intercepts of the correlation functions of the granular sources with coherent pion-emission decrease obviously compared to those with chaotic pion-emission droplets. The intercept decreases will become small with increasing droplet number  $n$ . However, the widths of two-pion correlation functions change slightly for the granular sources with chaotic and coherent pion-emission droplets.

We plot in Fig. 2 the four-pion correlation functions of the static granular sources with completely coherent pion-emission droplets. The parameters of the granular

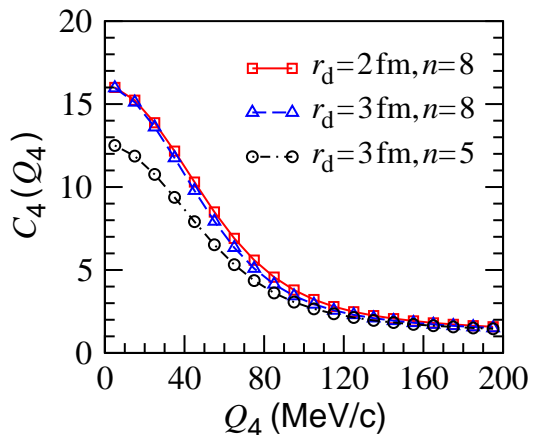


FIG. 2: (Color online) Four-pion correlation functions of the static granular sources with completely coherent pion-emission droplets. The parameters of the granular sources are the same as in Fig. 1.

sources are the same as in Fig. 1. The intercept of four-pion correlation function is sensitive to droplet number  $n$  in the granular source.

The normalized three-pion correlation function  $r_3$  is defined by the ratio of three-pion cumulant correlator to the square root of the product of the two-particle cor-

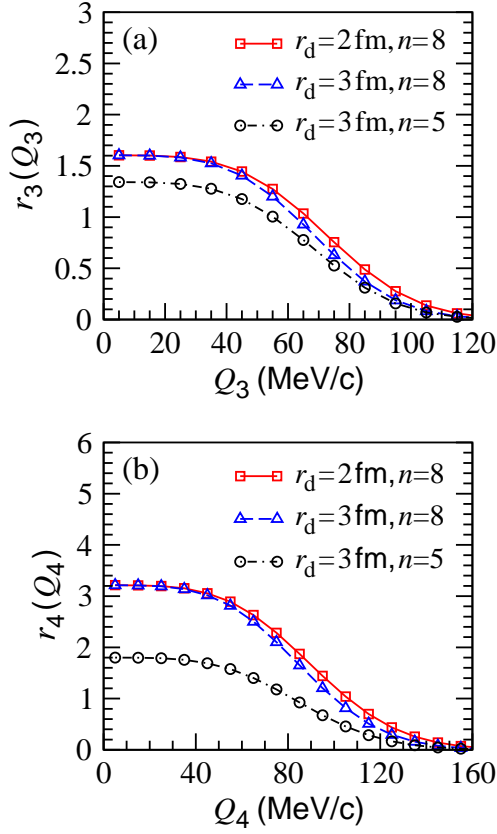


FIG. 3: (Color online) (a) Normalized three-pion correlation functions of the static granular sources with completely coherent pion-emission droplets. (b) Normalized four-pion correlation functions of the static granular sources with completely coherent pion-emission droplets. The parameters of the granular sources are the same as in Fig. 1.

relators [20]. For the granular source with completely coherent pion-emission droplets, it is given by

$$r_3(Q_3) = \frac{[c_3(Q_3) - 1][n/(n-1)]^{3/2}}{\sqrt{\mathcal{R}^G(1,2)(Q_3)\mathcal{R}^G(2,3)(Q_3)\mathcal{R}^G(1,3)(Q_3)}}, \quad (7)$$

where

$$c_3(Q_3) = 1 + \frac{2(n-1)(n-2)}{n^2} \times \left[ \mathcal{R}^G(1,2)\mathcal{R}^G(1,3)\mathcal{R}^G(2,3) \right]^{\frac{1}{2}}(Q_3). \quad (8)$$

Because  $r_3$  is insensitive to resonance decay, it is used to measure source coherence in analyses of experimental data [7, 22–24]. Similarly, the normalized four-pion correlation function  $r_4$  of the granular source is given by

$$r_4(Q_4) = \frac{[c_4(Q_4) - 1][n/(n-1)]^2}{\sqrt{\mathcal{R}^G(1,2)(Q_4)\mathcal{R}^G(2,3)(Q_4)\mathcal{R}^G(3,4)(Q_4)\mathcal{R}^G(1,4)(Q_4)}}, \quad (9)$$

where

$$c_4(Q_4) = 1 + \frac{2(n-1)(n-2)(n-3)}{n^3}$$

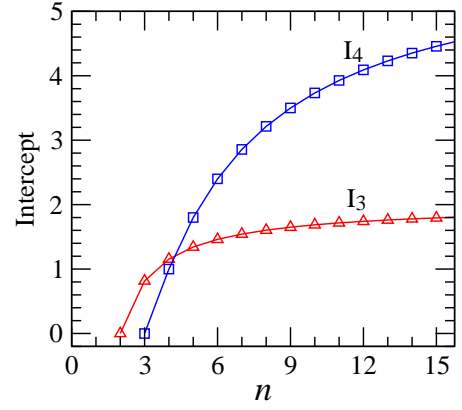


FIG. 4: (Color online) Intercepts of the  $r_3(Q_3)$  and  $r_4(Q_4)$  of the granular sources with completely coherent pion-emission droplets, as functions of the droplet number in the static granular sources.

$$\begin{aligned} & \times \left[ \left( \mathcal{R}^G(1,2)\mathcal{R}^G(2,3)\mathcal{R}^G(3,4)\mathcal{R}^G(1,4) \right)^{\frac{1}{2}}(Q_4) \right. \\ & + \left( \mathcal{R}^G(1,3)\mathcal{R}^G(2,3)\mathcal{R}^G(2,4)\mathcal{R}^G(1,4) \right)^{\frac{1}{2}}(Q_4) \\ & \left. + \left( \mathcal{R}^G(1,2)\mathcal{R}^G(2,4)\mathcal{R}^G(3,4)\mathcal{R}^G(1,3) \right)^{\frac{1}{2}}(Q_4) \right]. \quad (10) \end{aligned}$$

In Figs. 3(a) and 3(b), we plot the normalized three- and four-pion correlation functions  $r_3(Q_3)$  and  $r_4(Q_4)$  of the static granular sources with completely coherent pion-emission droplets, respectively. The parameters of the granular source are the same as in Fig. 1. The normalized correlation functions have plateaus in low  $Q_{3,4}$  regions to  $\sim 50$  MeV/c. We plot the intercepts of the  $r_3(Q_3)$  and  $r_4(Q_4)$  as functions of the droplet number in Fig. 4. The intercepts of four-pion normalized correlation functions are more sensitive to the droplet number  $n$  than three-pion normalized correlation functions in  $5 < n < 12$  region.

### III. MULTI-PION BECS IN EVOLVING GRANULAR SOURCE MODEL

The evolving granular source models can reproduce the pion transverse-momentum spectrum, elliptic flow, and interferometry radii [34–36]. We next investigate the multi-pion BECs for the evolving granular sources in which the droplets expand in viscous hydrodynamics and emit pions coherently.

#### A. Evolving granular source model

The model we consider is based on a viscous granular source model developed in Ref. [36], but here the pions emitted from one droplet is assumed completely or partially coherent. In this subsection, we present briefly the

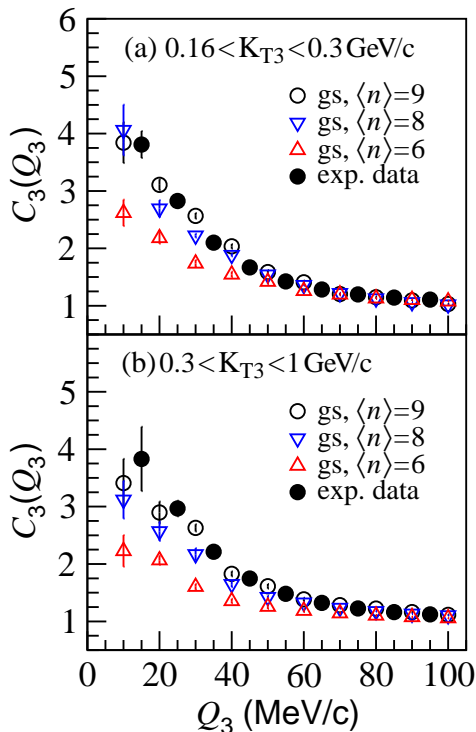


FIG. 5: (Color online) Comparisons of three-pion correlation functions of the evolving granular sources with completely coherent pion-emission droplets and the experimental data in central Pb-Pb collisions at  $\sqrt{s_{NN}} = 2.76$  TeV [8], in transverse-momentum intervals (a)  $0.16 < K_{T3} < 0.3$  GeV/c and (b)  $0.3 < K_{T3} < 1$  GeV/c. Here,  $\langle n \rangle$  denotes the average droplet number in the evolving granular sources.

ingredients of the granular source model used in the work. Some details of granular source models may refer to Refs. [28–30, 34–36].

In the granular source model, it is assumed that the initial spatial inhomogeneous and violent expansion at the early stages of the system produced in ultrarelativistic heavy-ion collisions may lead to a breakup of the system to many hot and dense droplets and form a granular particle-emitting source. At the formation time of the initial granular source, the droplet centers distribute within a cylinder along the collision axis. And, the initial energy distribution in a droplet satisfies a Woods-Saxon distribution as in Res. [35, 36]. The average droplet number,  $\langle n \rangle$ , of the granular source is related to the initial mean separation and geometry of the source [39].

The evolution of the granular source includes the droplet evolution in viscous hydrodynamics and the droplet expansion in whole with anisotropic droplet velocities  $v_{dx}$ ,  $v_{dy}$ , and  $v_{dz}$ . In the granular source model, the geometry and velocity parameters are determined by comparing the model results of pion transverse-momentum spectrum, elliptic flow, and two-pion interferometry radii with experimental data. In this paper, we use the viscous granular source model developed in Ref. [36] to describe the source evolution in Pb-Pb collisions

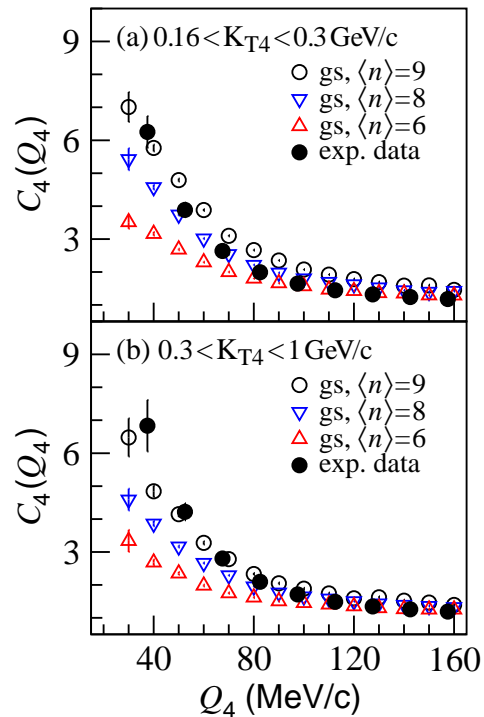


FIG. 6: (Color online) Comparison of four-pion correlation functions of the evolving granular sources with completely coherent pion-emission droplets and the experimental data in central Pb-Pb collisions at  $\sqrt{s_{NN}} = 2.76$  TeV [8], in transverse-momentum intervals (a)  $0.16 < K_{T4} < 0.3$  GeV/c and (b)  $0.3 < K_{T4} < 1$  GeV/c. Here,  $\langle n \rangle$  denotes the average droplet number in the evolving granular sources.

at  $\sqrt{s_{NN}} = 2.76$  TeV [8], and the model parameters are taken as the same in [36].

## B. Multi-pion correlation functions

In Fig. 5, we plot the three-pion correlation functions  $C_3(Q_3)$  of the evolving granular sources with completely coherent pion-emission droplets for central Pb-Pb collisions at  $\sqrt{s_{NN}} = 2.76$  TeV. The experimental data of  $C_3(Q_3)$  measured by ALICE Collaboration in central Pb-Pb collisions [8] are presented for comparison. The panels (a) and (b) show the results in the low and high transverse-momentum intervals  $0.16 < K_{T3} < 0.3$  GeV/c and  $0.3 < K_{T3} < 1$  GeV/c, respectively. Here,  $K_{T3} = |\mathbf{p}_{T1} + \mathbf{p}_{T2} + \mathbf{p}_{T3}|/3$ . The average droplet number  $\langle n \rangle$  for the simulation events with the granular source parameters determined together by the experimental data of transverse-momentum spectra, elliptic flow, and interferometry radii in 0%–10% Pb-Pb collisions [36] is 8. In Fig. 5, the results for  $\langle n \rangle = 9$  and  $\langle n \rangle = 6$  are calculated with the same granular source parameters but a smaller and larger initial mean separation. The granular source results in small  $Q_3$  region increase with increasing average droplet number  $\langle n \rangle$ . However, the results for  $\langle n \rangle = 8$



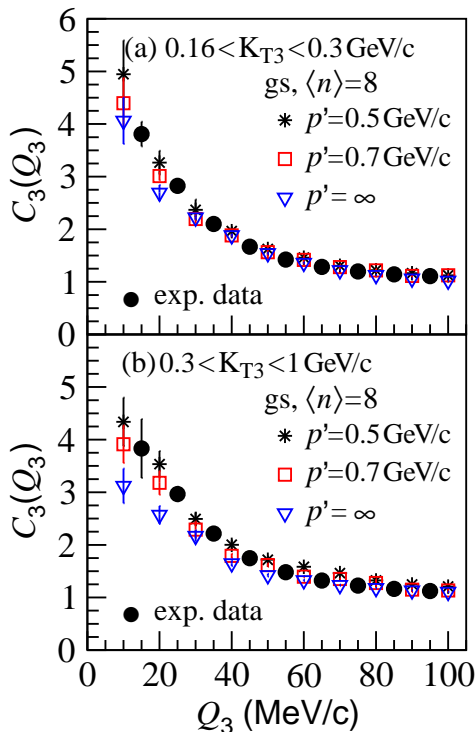


FIG. 7: (Color online) Three-pion correlation functions of the evolving granular sources with completely coherent ( $p' = \infty$ ) and partially coherent ( $p' = 0.5$  and  $0.7$  GeV/c) pion-emission droplets, in transverse-momentum intervals (a)  $0.16 < K_{T3} < 0.3$  GeV/c and (b)  $0.3 < K_{T3} < 1$  GeV/c. Here, the average droplet number of the granular source is 8 and the solid-circle symbols are the experimental data in central Pb-Pb collisions at  $\sqrt{s_{NN}} = 2.76$  TeV [8].

are lower than the experimental data in small  $Q_3$  region.

In Fig. 6, we plot the four-pion correlation functions  $C_4(Q_4)$  of the evolving granular sources with completely coherent pion-emission droplets for central Pb-Pb collisions at  $\sqrt{s_{NN}} = 2.76$  TeV. The experimental data of  $C_4(Q_4)$  measured by ALICE Collaboration in central Pb-Pb collisions [8] are presented for comparison. The panels (a) and (b) show the results in the low and high transverse-momentum intervals  $0.16 < K_{T4} < 0.3$  GeV/c and  $0.3 < K_{T4} < 1$  GeV/c, respectively. Here,  $K_{T4} = |\mathbf{p}_{T1} + \mathbf{p}_{T2} + \mathbf{p}_{T3} + \mathbf{p}_{T4}|/4$ . The four-pion correlation functions of the granular sources increase with increasing average droplet number  $\langle n \rangle$  in small  $Q_4$  region. And, the results for  $\langle n \rangle = 8$  are lower than the experimental data in small  $Q_4$  region.

Considering that the pions with high momenta are more possibly emitted chaotically from the excited-states [10, 11, 37, 38], we further investigate the multi-pion BECs for the granular sources with partially coherent pion-emission droplets. We assume that the pions emitted from one droplet and with momenta lower than a fixed value  $p'$  are amplitude coherent and therefore without intensity correlation. However, the pions with momenta higher than  $p'$  are chaotic emission (from excited-

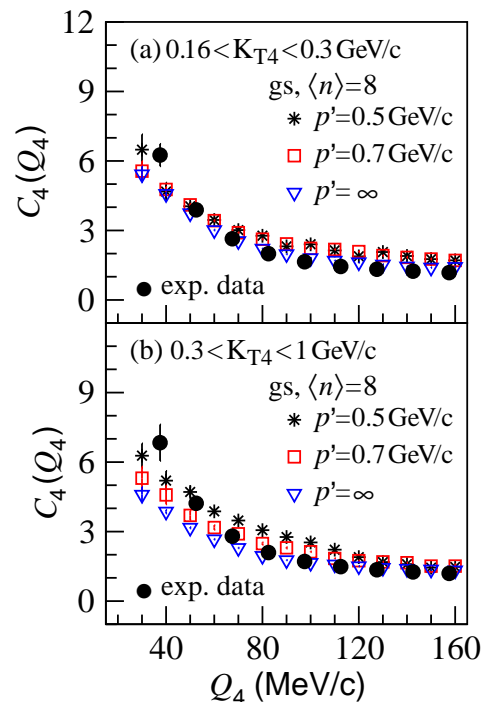


FIG. 8: (Color online) Four-pion correlation functions of the evolving granular sources with completely coherent ( $p' = \infty$ ) and partially coherent ( $p' = 0.5$  and  $0.7$  GeV/c) pion-emission droplets, in transverse-momentum intervals (a)  $0.16 < K_{T4} < 0.3$  GeV/c and (b)  $0.3 < K_{T4} < 1$  GeV/c. Here, the average droplet number of the granular source is 8 and the solid-circle symbols are the experimental data in central Pb-Pb collisions at  $\sqrt{s_{NN}} = 2.76$  TeV [8].

states).

In Figs. 7(a) and 7(b), we compare the three-pion correlation functions of the evolving granular sources with completely coherent pion-emission droplets (corresponding to  $p' = \infty$ ) and partially coherent pion-emission droplets with  $p' = 0.5$  and  $0.7$  GeV/c, in the lower and higher transverse-momentum  $K_{T3}$  intervals, respectively. Here, the average droplet number of the granular sources is 8 and the solid-circle symbols are the experimental data in central Pb-Pb collisions at  $\sqrt{s_{NN}} = 2.76$  TeV [8]. In low  $Q_3$  region, the three-pion correlation functions have an increase with decreasing  $p'$  and the increase is greater in the higher  $K_{T3}$  interval than in the lower  $K_{T3}$  interval. It is because that the contribution of chaotic pion emission in the correlation functions increases with decreasing  $p'$  and the pions with high momenta, which are more possibly emitted chaotically, have higher  $K_{T3}$  than those with low momenta. The three-pion correlation functions of the granular source with  $p' = 0.5$  GeV/c are approximately in agreement with the experimental data.

In Figs. 8(a) and 8(b), we compare the four-pion correlation functions of the evolving granular sources with completely coherent pion-emission droplets (corresponding to  $p' = \infty$ ) and partially coherent pion-emission

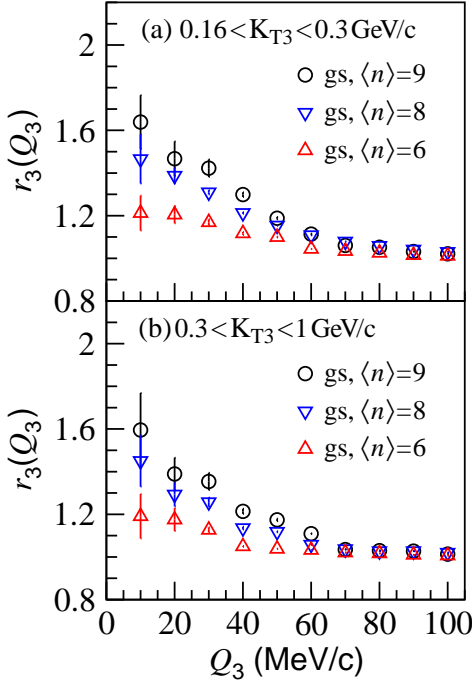


FIG. 9: (Color online) Normalized three-pion correlation functions of the evolving granular sources with completely coherent pion-emission droplets and the average droplet numbers  $\langle n \rangle = 9, 8,$  and  $6$ . (a)  $0.16 < K_{T3} < 0.3$  GeV/c and (b)  $0.3 < K_{T3} < 1$  GeV/c.

droplets with  $p' = 0.5$  and  $0.7$  GeV/c, in the lower and higher transverse-momentum  $K_{T4}$  intervals, respectively. Here, the average droplet number of the granular sources is  $8$  and the solid-circle symbols are the experimental data in central Pb-Pb collisions at  $\sqrt{s_{NN}} = 2.76$  TeV [8]. Compared to the three-pion correlation function in Fig. 7, the four-pion correlation function of granular source is more sensitive to the value of  $p'$ . However, it may needs more considerations to the momentum-dependence of coherent pion-emission from one droplet to let the multi-pion correlation functions of granular source agree with the experimental data.

### C. Normalized multi-pion BEC functions

The normalized multi-pion correlation functions  $r_3$  and  $r_4$  are believed suitable for analyzing the source coherence in relativistic heavy-ion collisions. We find in last section that the normalized correlation functions are sensitive to the droplet number in the static granular source with completely coherent pion-emission droplets. In this subsection we investigate the  $r_3$  and  $r_4$  in the evolving granular source with completely coherent and partially coherent pion-emission droplets.

We show in Figs. 9(a) and 9(b) the normalized three-pion correlation functions of the evolving granular sources with completely coherent pion-emission droplets

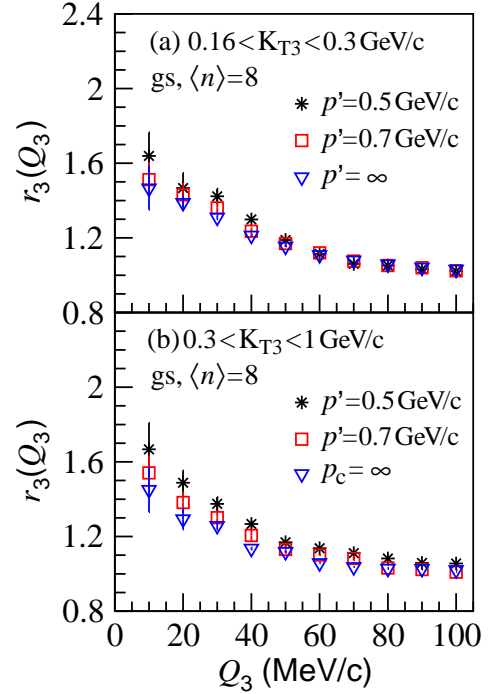


FIG. 10: (Color online) Comparison of the normalized three-pion correlation functions of the evolving granular sources with completely coherent ( $p' = \infty$ ) and partially coherent ( $p' = 0.5$  and  $0.7$  GeV/c) pion-emission droplets. (a)  $0.16 < K_{T3} < 0.3$  GeV/c and (b)  $0.3 < K_{T3} < 1$  GeV/c.

and the different values of average droplet number  $\langle n \rangle$  in the transverse-momentum intervals  $0.16 < K_{T3} < 0.3$  GeV/c and  $0.3 < K_{T3} < 1$  GeV/c, respectively. The normalized correlation function increases with increasing  $\langle n \rangle$  in both the transverse-momentum intervals. Compared to the normalized three-pion correlation functions of the static granular sources shown in Fig. 3(a), which have a plateau-structure in small  $Q_3$  region, the results of the evolving granular sources with the large  $\langle n \rangle$  values decrease with  $Q_3$  in small  $Q_3$  region. The decrease of  $r_3$  with increasing  $Q_3$  indicates that the three-pion cumulant correlator (correlation of pure pion-triplet interference) decrease more rapidly with increasing  $Q_3$  than two-pion correlations.

In Figs. 10, we compare the normalized three-pion correlation functions of the evolving granular sources with completely coherent ( $p' = \infty$ ) and partially coherent ( $p' = 0.5$  and  $0.7$  GeV/c) pion-emission droplets. Here, the average droplet number in the granular source is  $8$ . The normalized three-pion correlation functions increase slightly with decreasing value of  $p'$ . However, the intercepts of the correlation functions at  $Q_3 \sim 0$  are approximately in agreement, because the intercept is mainly determined by the droplet number in the granular source.

We show in Figs. 11(a) and 11(b) the normalized four-pion correlation functions of the evolving granular sources with completely coherent pion-emission droplets and the different values of average droplet number  $\langle n \rangle$

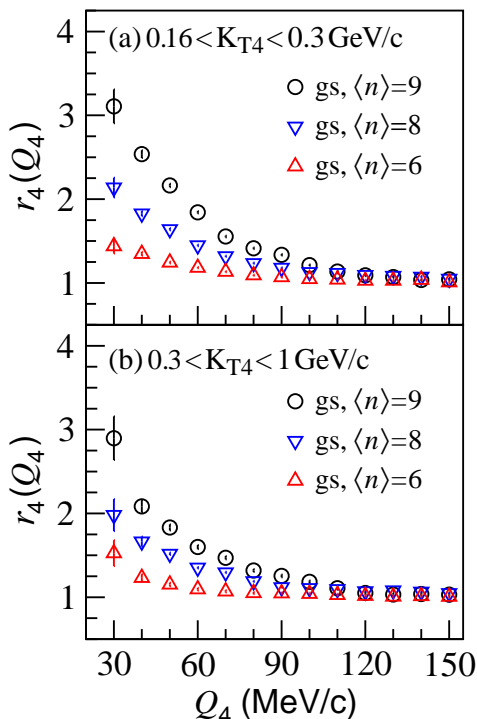


FIG. 11: (Color online) Normalized four-pion correlation functions of the evolving granular sources with completely coherent pion-emission droplets and the average droplet numbers  $\langle n \rangle = 9, 8$ , and  $6$ . (a)  $0.16 < K_{T4} < 0.3$  GeV/c and (b)  $0.3 < K_{T4} < 1$  GeV/c.

in the transverse-momentum intervals  $0.16 < K_{T4} < 0.3$  GeV/c and  $0.3 < K_{T4} < 1$  GeV/c, respectively. The normalized correlation function increases with increasing  $\langle n \rangle$  in both the transverse-momentum intervals. Compared to the normalized three-pion correlation functions of the evolving granular sources shown in Fig. 9, the four-pion correlation functions are more sensitive to  $\langle n \rangle$ .

In Figs. 12, we compare the normalized four-pion correlation functions of the evolving granular sources with completely coherent ( $p' = \infty$ ) and partially coherent ( $p' = 0.5$  and  $0.7$  GeV/c) pion-emission droplets. Here, the average droplet number in the granular source is  $8$ . The normalized four-pion correlation functions increase with decreasing value of  $p'$ . In the wide transverse-momentum interval,  $0.3 < K_{T4} < 1$  GeV/c, the normalized four-pion correlation function for the smallest  $p'$  has an obvious enhancement around  $Q_4 \sim 100$  MeV/c due to the momentum dependence of pion-emission coherence and the sensitivity of high-order pion correlations to source coherence. As discussed in Ref. [11], the average pion momentum will increase with increasing  $Q_4$  if there are no other constraints. This leads to an increase of chaotic emission possibility with increasing  $Q_4$  and the enhancement of  $r_4(Q_4)$  in middle  $Q_4$  region (see Fig. 7(d) in [11]). It is a signal of the pion coherent emission caused by identical boson condensation.

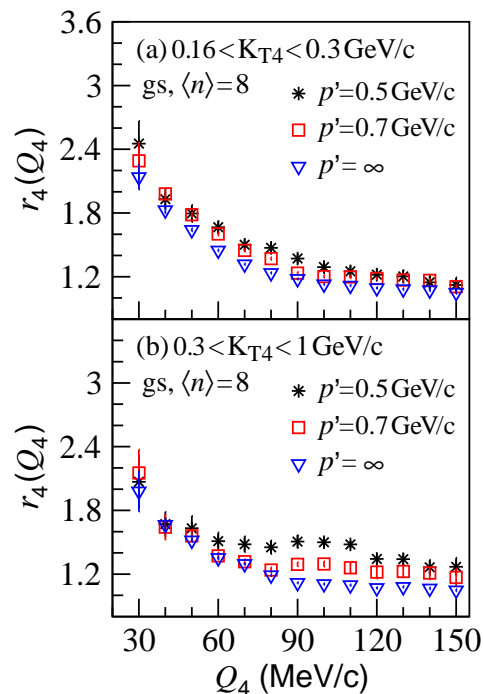


FIG. 12: (Color online) Comparison of the normalized four-pion correlation functions of the evolving granular sources with completely coherent ( $p' = \infty$ ) and partially coherent ( $p' = 0.5$  and  $0.7$  GeV/c) pion-emission droplets. (a)  $0.16 < K_{T4} < 0.3$  GeV/c and (b)  $0.3 < K_{T4} < 1$  GeV/c.

#### IV. SUMMARY AND DISCUSSION

We have investigated the three- and four-pion BECs in the granular source model with coherent pion-emission droplets. The multi-pion correlation functions and the normalized multi-pion correlation functions of the granular sources are examined for completely coherent and momentum-dependent partially coherent pion-emissions from a droplet, in the transverse-momentum intervals  $0.16 < K_{T3}, K_{T4} < 0.3$  GeV/c and  $0.3 < K_{T3}, K_{T4} < 1$  GeV/c. It is found that the intercepts of the multi-pion correlation functions at the relative momenta near zero are sensitive to the droplet number in the granular source. They decrease with decreasing droplet number. The three- and four-pion correlation functions of evolving granular sources are in basic agreement with recent experiment measurements carried out by the ALICE Collaboration in central Pb-Pb collisions at  $\sqrt{s_{NN}} = 2.76$  TeV. In the wide transverse momentum interval  $0.3 < K_{T4} < 1$  GeV/c, the normalized four-pion correlation function has an obvious enhancement in  $Q_4 \sim 100$  MeV/c region. This is a signal that high-momentum pions are more possibly emitted chaotically compared to low-momentum pions which may condense in the ground state due to identical boson condensation.

Compared to two-pion BEC, multi-pion BECs are more sensitive to the coherence of particle-emitting source. However, it is still an open question to extract



quantitatively the source coherence from multi-pion correlation functions. The main reasons are the absence of a fitting formula to the correlation functions with respect to the variables of relative momenta, the influence of other effects on the correlation functions in the small variable regions of relative momenta, and the limited statistics in the small variable regions. The normalized multi-pion correlation functions, defined as the ratios of the multi-pion cumulant correlators to two-pion correlator, can reduce the influence of resonance decay on themselves. They exhibit a plateau structure in the small variable regions of relative momenta for the static sources. However, whether the plateau structure can still remain for expanding sources and how to get the intercepts of  $r_3$  and  $r_4$  at the zero relative-momentum variables will be interesting issues.

Finally, it should be mentioned that the granular source model we used in this paper with the same model parameters as in Ref. [36] but with the assumption of

coherent pion emission from one droplet. We noted that this assumption may increase the two-pion interferometry radii by  $\sim 4\%$  averagely and decrease the two-pion chaoticity parameter  $\lambda$  by  $\sim 10\%$ . However, the assumption of coherent pion emission hardly changes the results of the transverse-momentum spectrum and elliptic flow. Considering more realistic momentum-dependent coherent emission of pions in a droplet and investigating the multi-pion BECs in the more realistic model will be of interest.

### Acknowledgments

This research was supported by the National Natural Science Foundation of China under Grant Nos. 11675034 and 11275037.

- 
- [1] M. Gyulassy, S. K. Kauffmann, and Lance W. Wilson, Phys. Rev. C **20**, 2267 (1979).
- [2] C. Y. Wong, *Introduction to High-Energy Heavy-Ion Collisions* (World Scientific, Singapore, 1994), Chap. 17.
- [3] U. A. Wienemann and U. Heinz, Phys. Rep. **319**, 145 (1999).
- [4] R. M. Weiner, Phys. Rep. **327**, 249 (2000).
- [5] T. Csörgő, Heavy Ion Physics **15** (2002) 1; arXiv:hep-ph/0001233.
- [6] M. A. Lisa, S. Pratt, R. Soltz, and U. Wiedemann, Annu. Rev. Nucl. Part. Sci. **55**, 357 (2005).
- [7] B. Abelev et al. (ALICE Collaboration), Phys. Rev. C **89** (2014) 024911.
- [8] J. Adam et al. (ALICE Collaboration), Phys. Rev. C **93** (2016) 054908.
- [9] D. Gangadharan, Phys. Rev. C **92** (2015) 014902.
- [10] G. Bary, P. Ru, and W. N. Zhang, J. Phys. G **45** (2018) 065102.
- [11] G. Bary, P. Ru, and W. N. Zhang, J. Phys. G **46** (2019) 115107.
- [12] Y. M. Liu, D. Beavis, S. Y. Chu, S. Y. Fung, D. Keane, G. VanDalen, and M. Vient, Phys. Rev. C **34** (1986) 1667.
- [13] W. A. Zajc, Phys. Rev. D **35**, (1987) 3396.
- [14] M. Biyajima, A. Bartl, T. Mizoguchi, N. Suzuki and O. Terazawa, Prog. Theor. Phys. **84** (1990) 931.
- [15] I. V. Andreev, M. Plümer, R. M. Weiner, Phys. Rev. Lett. **67**, (1991) 3475; I. V. Andreev, M. Plümer, R. M. Weiner, Int. J. Mod. Phys. **A8**, (1993) 4577.
- [16] S. Pratt, Phys. Lett. B **301** (1993) 159.
- [17] T. Csörgő and J. Zimányi, Phys. Rev. Lett. **80** (1998) 916; J. Zimányi and T. Csörgő, Heavy Ion Physics **9** (1999) 241; arXiv:hep-ph/9705432.
- [18] W. N. Zhang, Y. M. Liu, S. Wang *et al.*, Phys. Rev. **C47**, (1993) 795; W. N. Zhang, Y. M. Liu, L. Huo *et al.*, Phys. Rev. **C51**, (1995) 922; W. N. Zhang, L. Huo, X. J. Chen *et al.*, Phys. Rev. **C58**, (1998) 2311; W. N. Zhang, G. X. Tang, X. J. Chen *et al.*, Phys. Rev. **C62**, (2000) 044903.
- [19] W. Q. Chao, C. S. Gao, and Q. H. Zhang, J. Phys. **G21**, (1995) 847; Q. H. Zhang, W. Q. Chao, and C. S. Gao, Phys. Rev. **C52**, (1995) 2064.
- [20] U. Heinz and Q. H. Zhang, Phys. Rev. C **56** (1997) 426; U. Heinz and A. Sugarbaker, Phys. Rev. C **70** (2004) 054908.
- [21] H. Nakamura and R. Seki, Phys. Rev. **C60**, (1999) 064904; H. Nakamura and R. Seki, Phys. Rev. **C61**, (2000) 054905.
- [22] H. Bøggild et al. (NA44 Collaboration), Phys. Lett. B **455** (1999) 77; I. G. Bearden et al. (NA44 Collaboration), Phys. Lett. B **517** (2001) 25.
- [23] M. M. Aggarwa et al. (WA98 Collaboration), Phys. Rev. Lett. **85** (2000) 2895; M. M. Aggarwa et al. (WA98 Collaboration), Phys. Rev. C **67** (2003) 014906.
- [24] J. Adams et al. (STAR Collaboration), Phys. Rev. Lett. **91** (2003) 262301.
- [25] M. Csanáda for the PHENIX Collaboration, Nucl. Phys. A **774** (2006) 611.
- [26] K. Morita, S. Muroya, and H. Nakamura, Prog. Theor. Phys. **116** (2006) 329.
- [27] W. N. Zhang, M. J. Efaaf, C. Y. Wong, Phys. Rev. C **70** (2004) 024903.
- [28] W. N. Zhang, Y. Y. Ren, and C. Y. Wong, Phys. Rev. C **74** (2006) 024908.
- [29] W. N. Zhang, Z. T. Yang, and Y. Y. Ren, Phys. Rev. C **80** (2009) 044908.
- [30] W. N. Zhang, H. J. Yin, and Y. Y. Ren, Chin. Phys. Lett. **28** (2011) 122501.
- [31] S. S. Adler *et al.* (PHENIX Collaboration), Phys. Rev. Lett. **93** (2004) 152302.
- [32] J. Adams *et al.* (STAR Collaboration), Phys. Rev. **71** (2005) 044906.
- [33] K. Aamodt *et al.* (ALICE Collaboration), Phys. Lett. B **696** (2011) 328.
- [34] J. Yang, Y. Y. Ren, and W. N. Zhang, Advances in High Energy Physics, **2015** (2015) 846154.
- [35] J. Yang, Y. Y. Ren, and W. N. Zhang, in Proceeding of the Xth Workshop on Particle Correlations and Femtoscopy (WPCF14) (Gyöngyös, Hungary on Aug. 2014);

- arXiv:1501.03651[nucl-th].
- [36] J. Yang, W. N. Zhang, and Y. Y. Ren, Chinese Physics C **41** (2017) 084102.
- [37] C. Y. Wong and W. N. Zhang, Phys. Rev. C **76** (2007) 034905.
- [38] J. Liu, P. Ru, W. N. Zhang, C. Y. Wong, J. Phys. G **41** (2014) 125101.
- [39] S. Pratt, P. J. Siemens, and A. P. Vischer, Phys. Rev. Lett. **68** (1992) 1109.
- [40] W. N. Zhang, Y. M. Liu, L. Huo, Y. Z. Jiang, D. Keane, and S. Y. Fung, Phys. Rev. C **51** (1995) 922.